

## Human Low-Molecular-Weight Salivary Mucin Expresses the Sialyl Lewis<sup>x</sup> Determinant and Has L-Selectin Ligand Activity<sup>†</sup>

Akraporn Prakobphol,<sup>‡</sup> Kristina A. Thomsson,<sup>§</sup> Gunnar C. Hansson,<sup>§</sup> Steven D. Rosen,<sup>||</sup> Mark S. Singer,<sup>||</sup> Nancy J. Phillips,<sup>⊥</sup> Katalin F. Medzihradszky,<sup>⊥</sup> Alma L. Burlingame,<sup>⊥</sup> Hakon Leffler,<sup>⊥,▽</sup> and Susan J. Fisher<sup>\*,‡,||,⊥,Ⓢ</sup>

Departments of Stomatology, Anatomy, Pharmaceutical Chemistry, Psychiatry, and Obstetrics, Gynecology and Reproductive Sciences, University of California, San Francisco, San Francisco, California 94143, and Department of Medical Biochemistry, Göteborg University, Göteborg, Sweden

Received October 22, 1997; Revised Manuscript Received January 9, 1998

**ABSTRACT:** Previously we showed that the low-molecular-weight mucin (MG2, encoded by *MUC7*), a major component of human submandibular/sublingual saliva, is a bacterial receptor that coats the tooth surface. Here we tested the hypothesis that the structure of its carbohydrate residues contains important information about its function. Purified MG2 (*M<sub>r</sub>* 120 000) was digested with trypsin, and the resulting *M<sub>r</sub>* 90 000 fragment, which carried primarily O-linked oligosaccharides, was subjected to reductive  $\beta$ -elimination. The released oligosaccharides were characterized by using nuclear magnetic resonance spectroscopy and mass spectrometry. Of the 41 different structures we detected, the most prominent included NeuAc $\alpha$ 2 $\rightarrow$ 3Gal $\beta$ 1 $\rightarrow$ 3GalNAc-ol (sialyl-T antigen), Gal $\beta$ 1 $\rightarrow$ 4(Fuc $\alpha$ 1 $\rightarrow$ 3)GlcNAc $\beta$ 1 $\rightarrow$ 6-(Gal $\beta$ 1 $\rightarrow$ 3)GalNAc-ol [type 2 core with Lewis<sup>x</sup> (Le<sup>x</sup>) determinant], and NeuAc $\alpha$ 2 $\rightarrow$ 3Gal $\beta$ 1 $\rightarrow$ 4(Fuc $\alpha$ 1 $\rightarrow$ 3)-GlcNAc $\beta$ 1 $\rightarrow$ 6(Gal $\beta$ 1 $\rightarrow$ 3)GalNAc-ol [type 2 core with sialyl Le<sup>x</sup> (sLe<sup>x</sup>) determinant]. We also detected di-, tri-, and pentasaccharides with one sulfate group. Le<sup>x</sup>, sLe<sup>x</sup>, and related sulfated structures are ligands for selectins, adhesion molecules that mediate leukocyte trafficking. Therefore, we investigated whether MG2 was a selectin ligand. In an enzyme-linked immunosorbent assay, L-selectin chimeras interacted with immobilized MG2 in a Ca<sup>2+</sup>-dependent manner. L-Selectin chimeras also bound to MG2 immobilized on nitrocellulose. Together, these results suggest that the saccharides that MG2 carries could specify some of its important functions, which may include mediating leukocyte interactions in the oral cavity.

Human saliva has several critical functions. In addition to its long-recognized role in lubrication (1–3) and digestion (4), saliva also forms a bioactive, semipermeable barrier [i.e., pellicle (5–7)] that coats oral surfaces, where it helps prevent demineralization (8, 9). Saliva also plays a role in regulating the oral flora, either by virtue of its antimicrobial activity (10, 11) or by promoting selective microbial clearance or adherence (12–15).

The diverse functions attributed to saliva are apportioned among its many components. These have been classified into several families of structurally related molecules:

amylases, cystatins, proline-rich proteins, proline-rich glycoproteins, carbonic anhydrases, peroxidases, statherins, histatins, lactoferrin, lysozyme, sIgA, and mucins. To date, the complete protein sequences of all the major salivary constituents, except the high-molecular-weight mucin (MG1),<sup>1</sup> have been deduced from the nucleotide sequences of the corresponding genes (16–20). This has allowed investigators to correlate particular peptide sequences within the protein portion of these molecules with specific functions (20–22).

In contrast, relatively little is known about the structures of the carbohydrate residues that salivary glycoproteins carry. Our previous work suggests that the saccharide portions of these molecules play a particularly important role in specifying the unique repertoire of bacterial species with which each salivary glycoprotein interacts. We found, by overlaying nitrocellulose blots of electrophoretically separated salivary glycoproteins with bacteria, that there is a great deal of specificity in the interactions we observed (12, 13). For

<sup>†</sup> This work was supported by grants from the National Institutes of Health (DE 07244, RR 01614, and GM23547), the National Science Foundation (Biological Instrumentation Program Grant DIR 8700766), and the IngaBritt and Arne Lundbergs Foundation, Swedish Medical Research Council (Nos. 7461 and 10446). Some of the mass spectrometers were obtained by grants from FRN and the Knut and Alice Wallenberg foundation and supported by the Swedish Medical Research Council (No. 3967).

\* Corresponding author: HSW 604, University of California San Francisco, San Francisco, CA 94143-0512. Telephone: (415) 476-5297. Fax: (415) 476-4204. E-mail: sfisher@cgl.ucsf.edu.

<sup>‡</sup> Department of Stomatology, University of California, San Francisco.

<sup>§</sup> Department of Medical Biochemistry, Göteborg University.

<sup>||</sup> Department of Anatomy, University of California, San Francisco.

<sup>⊥</sup> Department of Pharmaceutical Chemistry, University of California, San Francisco.

<sup>▽</sup> Department of Psychiatry, University of California, San Francisco.

<sup>Ⓢ</sup> Department of Obstetrics, Gynecology, and Reproductive Sciences, University of California, San Francisco.

<sup>1</sup> Abbreviations: MG1, high-molecular-weight salivary mucin; MG2, low-molecular-weight salivary mucin; gPRP, highly glycosylated proline-rich glycoprotein; NMR, nuclear magnetic resonance; SMSL, submandibular/sublingual; sLe<sup>x</sup>, sialyl Lewis<sup>x</sup> determinant; ECL, enhanced chemiluminescence; MG2-T90, tryptic fragment of MG2, *M<sub>r</sub>* 90 000, carrying O-linked oligosaccharides; DQF-COSY, double quantum-filtered correlated spectroscopy; MALDI-TOFMS, matrix-assisted laser desorption/ionization time-of-flight mass spectrometry; GC-EIMS, gas chromatography–electron impact mass spectrometry; FABMS, fast atom bombardment mass spectrometry.

example, *Fusobacterium nucleatum*, a periodontal pathogen, adheres primarily to the highly glycosylated proline-rich glycoprotein (gPRP), the major glycosylated component of human parotid saliva. Subsequently, we found that this interaction is mediated by the carbohydrate portion of the molecule. Using a combination of NMR spectroscopy and mass spectrometry, we discovered that an unusual, bi-antennary N-linked saccharide, which carries the Lewis y (Le<sup>y</sup>) determinant [(Fuc $\alpha$ 1 $\rightarrow$ 2)Gal $\beta$ 1 $\rightarrow$ 4(Fuc $\alpha$ 1 $\rightarrow$ 3)-GlcNAc $\beta$ 1)], is the most abundant gPRG oligosaccharide species (12). Immunoblotting with a Le<sup>y</sup>-specific antibody showed that, among salivary glycoproteins, expression of this epitope is confined primarily to the gPRP (unpublished data). Together, these results suggest that individual salivary glycoproteins carry unique oligosaccharide structures and that this lack of redundancy among oligosaccharide structures could restrict the repertoire of bacteria with which these glycoproteins interact.

We have also been interested in the role that specific oligosaccharide species play in functions mediated by the salivary mucins, the major glycosylated components of human submandibular/sublingual (SMSL) saliva. This family of salivary glycoproteins has two members: the high-molecular-weight mucin encoded by *MUC5B* [MG1,  $M_r$  >1 000 000 (23)] and the low-molecular-weight mucin encoded by *MUC7* [MG2,  $M_r$  120 000 (19)]. Studies of the purified mucins also indicate that they are structurally distinct. MG1, which contains 15% protein and 78% carbohydrate, consists of large, disulfide-linked peptide subunits (24, 25). In contrast, MG2, which contains 30% protein and 68% carbohydrate, exists as a much smaller, single peptide chain (24–26). Our work suggests that both MG1 and MG2 are major components of the salivary pellicle that coats the tooth surface (27), but they differ greatly in the species of bacteria with which they interact (13).

As with other salivary glycoproteins, a great deal is known about the peptide repeats that form the MG1 and MG2 cores. Comparison of the amino acid sequences encoded by the full-length *MUC7* gene (19) and fragments of the *MUC5B* gene (23, 28), together with information obtained by Edman degradation, suggests that MG2 contains higher amounts of threonine, serine, proline, and alanine than MG1 (24). Relatively less is known about the carbohydrate structures that MG1 and MG2 carry. We initiated a detailed characterization of the specific saccharide species carried by MG2 with the goal of determining the structural features of the carbohydrate residues that specify the molecule's bacterial receptor activity. Surprisingly, we discovered that potential selectin ligands (Le<sup>x</sup>, sLe<sup>x</sup>, and related sulfated structures) were prominent among the MG2 saccharide species. In additional experiments we confirmed that these saccharides allow MG2 to serve as a selectin ligand, thus suggesting a novel function for this major salivary glycoprotein.

## EXPERIMENTAL PROCEDURES

**Materials.** All chemicals, unless otherwise noted, were obtained from Sigma Chemical Co., St. Louis, MO. Nitrocellulose membrane (0.45  $\mu$ m) was obtained from Schleicher & Schuell, Keene, NH. Enhanced chemiluminescence (ECL) detection reagents, Hyperfilm ECL and Hyperfilm  $\beta$ max, were products of Amersham, Arlington Heights, IL. TPCK

modified trypsin (sequencing grade) was from Promega, Madison, WI. Monoclonal antibodies CSLEX-1 (ascites) and 2H-5 (conditioned medium), which recognize the sLe<sup>x</sup> epitope, were gifts from Dr. L. Stoolman, University of Michigan, Ann Arbor, MI, and Dr. R. Kannagi, Aichi Cancer Center, Nagoya, Japan, respectively. The mouse L-selectin/human IgG chimera-secreting cell line was a gift from Dr. L. Lasky, Genentech Inc., South San Francisco, CA. Horse-radish peroxidase-conjugated goat anti-mouse IgM heavy and light chains, normal mouse serum, and normal goat serum were from Jackson Immuno Research Laboratories Inc., West Grove, PA. Vectastain ABC reagents, biotinylated lectins (jacalin and wheat germ agglutinin), and bacterial alkaline phosphatase substrate kit II were from Vector Laboratories, Burlingame, CA. Immulon 2 plates were from Dynatech Laboratories, Chantilly, VA. Biotinylated goat anti-human IgG (Fc-specific) and streptavidin-alkaline phosphatase were from Caltag, South San Francisco, CA.

**Collection of SMSL Saliva and Isolation of MG2.** Human SMSL saliva was collected on ice as the ductal secretion from a donor who was a secretor with blood type B+, Le (a–b–). The sample was diluted with an equal volume of cold PBS, clarified by centrifugation, dialyzed against distilled water at 4 °C overnight, and lyophilized. The lyophilized sample (10 mg) was dissolved in 2 mL of loading buffer, pH 7.0, containing 6 M urea, 1% SDS, and 1%  $\beta$ -mercaptoethanol. After centrifugation to remove undissolved material, the sample was subjected to preparative SDS–PAGE, using a model 491 Prep Cell (Bio-Rad Laboratories). The acrylamide concentration that best separated the MG2 ( $M_r$  120 000) from contaminants of similar molecular weight was determined, by using analytical slab SDS–PAGE, to be 5% for the resolving gel and 3% for the stacking gel. The electrophoretically separated proteins were continuously eluted from the preparative gel and collected into fractions by pumping through the elution chamber. Fractions containing MG2, as determined by analytical SDS–PAGE, were pooled and dialyzed extensively, first against PBS containing 0.5 M NaCl and then against distilled water. The dialyzed sample was concentrated by lyophilization, and purity was assessed by analytical SDS–PAGE and staining either with silver (29) or with alcian blue followed by silver to enhance detection of glycosylated proteins (30). If the resulting MG2 contained contaminants, the sample was re-electrophoresed using the preparative gel system described above until homogeneity was achieved.

**Preparation of the MG2-T90 Tryptic Fragment.** The MG2 sample (4.0 mg) was digested with TPCK modified trypsin (200  $\mu$ g) as described (31). The large tryptic fragment that carried the O-linked oligosaccharides (hereafter referred to as MG2-T90) was separated from other smaller peptides by size-exclusion chromatography on a Superdex 75 HR column (Pharmacia).

**Release of Oligosaccharides from MG2-T90 and Separation of the Neutral, Sialylated, and Sulfated O-Linked Oligosaccharide Fractions.** The O-linked oligosaccharides were released from MG2-T90 (1.3 mg) by reductive  $\beta$ -elimination in 0.05 M NaOH/1M NaBH<sub>4</sub> (1 mL) for 48 h at 50 °C. Excess borate was removed by codistillation of borate methyl ester with methanol/1% acetic acid followed by desalting on Dowex 50WX8. The released oligosaccharide mixture was first analyzed by 1-D and 2-D (DQF-COSY) proton

NMR spectroscopy (see below). A portion of the saccharide mixture was then separated into neutral, sialylated, and sulfated fractions by anion-exchange chromatography as described (32).

**Analytical Methods.** The carbohydrate composition of purified MG2, MG2-T90, and the neutral, sialylated, and sulfated saccharide fractions was determined by high pH anion-exchange chromatography on a Dionex HPLC system equipped with a pulsed amperometric detector (Dionex, Sunnyvale, CA) as described (33, 34). N-Terminal amino acid sequences were determined by using an Applied Biosystems model 470A sequencer.

**NMR Spectroscopy.** The total oligosaccharide mixture recovered from reductive  $\beta$ -elimination of the MG2-T90 was dissolved in 0.3 mL D<sub>2</sub>O (99.996%; Cambridge Isotope Laboratories, Andover, MA). After repeated exchange by lyophilizing and redissolving in D<sub>2</sub>O, the sample was transferred to a 5-mm NMR tube. 1-D and 2-D <sup>1</sup>H NMR spectra were recorded on a 500-MHz NMR spectrometer (GN500, General Electric). 1-D <sup>1</sup>H spectra were recorded with 256 acquisitions at 25 and 52 °C. The phase-sensitive (TPPI) double quantum filtered correlated spectroscopy (DQF-COSY) (35, 36) analysis was recorded at 25 °C with 800 data points, 16 scans each in  $t_1$ , 2048 data points in  $t_2$ , and spectral width  $\pm 1500$  Hz. The data set was processed by using Striker software and displayed using Sparky software. Both programs were developed at the University of California, San Francisco, NMR facility (37–39). The data were transformed using apodization with a 45° shifted sine-bell window and 2K zero-filling. Chemical shifts were determined relative to acetone ( $\delta = 2.225$  ppm) used as an internal standard in a separate 1-D experiment. Signals were assigned to chemical reporter groups by comparison with published spectra of known structures (40, 41) and by the fine structure and location of cross-peaks in the DQF-COSY.

**Mass Spectrometry.** An aliquot of the underivatized oligosaccharide mixture, obtained after reductive  $\beta$ -elimination, was analyzed by matrix-assisted laser desorption ionization time-of-flight mass spectrometry (MALDI-TOFMS) on a Voyager Elite mass spectrometer (Perseptive Biosystems, Framingham, MA) in linear positive ion mode with delayed extraction. The matrix was prepared by mixing 0.2 M 2,5-dihydroxybenzoic acid and 0.06 M 1-hydroxyisoquinoline in 50% water/acetonitrile (1:1, v/v) (42). The neutral and sialylated oligosaccharides were permethylated and analyzed by MALDI-TOFMS on a VG TOF Spec E (Micromass, Manchester, U.K.). The matrix was prepared by mixing 2,5-dihydroxybenzoic acid (4  $\mu$ L, 0.05 M in 1:1 H<sub>2</sub>O/acetonitrile), LiCl (2  $\mu$ L, 0.05 M in H<sub>2</sub>O), and analyte (2  $\mu$ L, ethyl acetate).

In addition, the permethylated neutral and sialylated saccharide fractions were analyzed as previously described by using high-temperature gas chromatography–electron impact mass spectrometry (GC–EIMS) (43). The sulfated saccharides were perdeuteracetylated and analyzed by fast atom bombardment mass spectrometry (FABMS) according to published methods (44).

**SDS–PAGE and Transfer of Proteins.** Ductal SMSL saliva samples collected from 6 donors as described above and whole saliva samples collected from 26 donors by expectoration were mixed with an equal volume of loading buffer and stored frozen at –20 °C. These samples and

purified MG2 were electrophoresed on 7.5% or 10% slab gels (45), and the proteins were visualized by staining with silver (29) or with alcian blue followed by silver (30). Proteins from identical gels were transferred by blotting to nitrocellulose membranes (46).

**Western Blot Analyses.** For immunoblotting, nonspecific binding was blocked by incubating blots for 1 h in PBS containing 0.1% Tween-20 (T-PBS) and 5% Carnation nonfat dried milk (5% T-blotto). The blot was then incubated for 2 h with either the CSLEX-1 or the 2H-5 mAb diluted in 5% T-blotto at 1:100 and 1:20, respectively. The blot was washed in T-PBS as described above and then incubated for 1 h in horseradish peroxidase-conjugated goat anti-mouse IgM heavy and light chains diluted in 5% T-blotto. After washing, blots were immersed in ECL detection reagents, and the bands that interacted with the antibody were detected by exposing the blots to Hyperfilm ECL.

For assessing lectin binding to nitrocellulose transfers, nonspecific reactivity was blocked by incubating the blots for 1 h in 0.025 M Tris-HCl containing 0.5 M NaCl and 0.5% Nonidet P-40. The blots were then incubated in either biotinylated jacalin or biotinylated wheat germ agglutinin for 1 h, washed in the blocking buffer (3 times for 15 min), and incubated for 0.5 h in avidin and biotinylated horseradish peroxidase. The blot was washed and then immersed in ECL detection reagents for 1 min. Bands to which lectins bound were detected as described above.

**Binding of L-Selectin to MG2.** Two different techniques were used to examine L-selectin binding to MG2. In the first technique, wells of Immulon 2 plates were coated with MG2 by incubation (overnight at 4 °C) with purified mucin diluted 1  $\mu$ g/100  $\mu$ L in Dulbecco's PBS containing 0.02% NaN<sub>3</sub>. The wells were washed 3 times with T-PBS. Nonspecific binding was prevented by incubating the wells with 3% BSA in PBS (BSA–PBS) for 2 h at room temperature. Afterward, a preformed complex of L-selectin/human IgG chimeras, biotinylated goat anti-human IgG (Fc-specific), and streptavidin–alkaline phosphatase (0.1  $\mu$ g each in 100  $\mu$ L of BSA–PBS) (47) was added. Binding was allowed for 30 min at room temperature with gentle swirling. After the plate was washed (3 times in PBS), *p*-nitrophenyl phosphate (100  $\mu$ g in 100  $\mu$ L of 10% diethanolamine, pH 9.8, containing 0.5 mM MgCl<sub>2</sub> and 0.02% NaN<sub>3</sub>) was added to each well. After the color developed, the optical density at 405 nm was determined by using a microplate reader (Bio-Rad Laboratories). As a control for specificity, binding in the presence of 10 mM EDTA was also assessed. This experiment was repeated twice.

In the second technique, SMSL or whole saliva samples obtained from individual donors were electrophoretically separated and transferred to a nitrocellulose membrane as described above. Nonspecific binding was blocked by incubating the membrane in 5% T-blotto for 1 h at room temperature. Then the blot was overlaid with a preformed complex of L-selectin/human IgG chimeras, biotinylated goat anti-human IgG, and streptavidin–alkaline phosphatase suspended in 5% T-blotto as described above. An identical control blot was incubated in the presence of 10 mM EDTA. After the blots were washed in T-PBS (3 times for 5 min), the selectin-reactive bands were visualized by staining the blot with bacterial alkaline phosphatase substrate kit II according to the manufacturer's instructions.

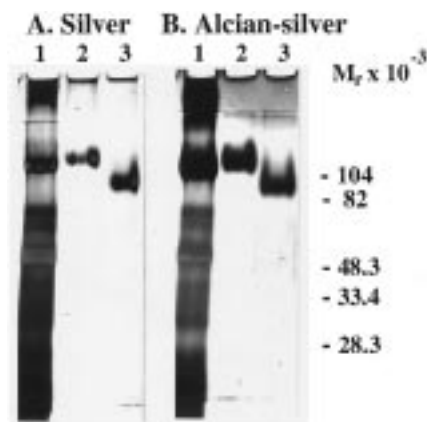


FIGURE 1: Isolation of MG2 from SMSL saliva and preparation of the MG2-T90 tryptic fragment. Lane 1 contained SMSL saliva before purification; lane 2, the purified MG2; and lane 3, the  $M_r$  90 000 MG2 tryptic fragment (MG2-T90). Gel A was stained with silver to detect proteins, and gel B was stained with alcian blue followed by silver to enhance detection of glycoproteins.

## RESULTS

**Isolation of MG2-T90.** The amino acid sequence of MG2, which has been deduced from the corresponding gene (*MUC7*), shows that the potential O-glycosylation sites are clustered on tandem repeats near the carboxyl terminus, while the potential N-glycosylation sites are at the amino terminus (19). Trypsin digestion of intact MG2 produces a large,  $M_r$  90 000 fragment (MG2-T90) that contains the C-terminal tandem repeats (31). Therefore, we isolated the region of the molecule that contains O-linked saccharides by purifying MG2 from a SMSL saliva sample collected from a single individual, subjecting the purified MG2 to trypsin proteolysis, and isolating the high-molecular-weight product by size-exclusion chromatography. All three fractions were analyzed by SDS-PAGE (Figure 1). Before purification, the SMSL saliva sample contained many components (lane 1). After purification, the MG2 fraction consisted of a single  $M_r$  120 000 glycoprotein (lane 2). Size-exclusion chromatography of the trypsin digest resulted in a single high-molecular-weight peak, which contained only the  $M_r$  90 000 MG2 glycoprotein fragment (lane 3). The N-terminal amino acid sequence of the purified MG2 was determined. Except for the underlined residues, the sequence LHKRSRP-KLPPSPNNPP was found to be identical to the predicted N-terminal sequence of the mature protein encoded by *MUC7* (19). The N-terminal amino acid sequence of MG2-T90 (ENVXTXSSV) showed that trypsin cleavage occurred at the expected site. Together, these results show that we purified the portion of MG2 that carries most of the O-linked saccharides.

**Monosaccharide Composition of MG2-T90.** The O-linked oligosaccharides were released from MG2-T90 by reductive  $\beta$ -elimination. After desalting, the entire oligosaccharide mixture was analyzed by NMR spectroscopy, described next. An aliquot was then removed for MALDI-TOFMS analysis, also described below. The remainder was fractionated into neutral, sialylated, and sulfated species by DEAE ion-exchange chromatography as previously described (32). In brief, the neutral oligosaccharides were eluted directly, and the remaining fraction, which bound to the column, was treated with iodomethane in DMSO to convert carboxyl

groups into methyl esters. As a result, the sialic acid-containing oligosaccharides were converted into neutral species that no longer interacted with the column. The remaining sulfated oligosaccharides ( $\pm$ sialic acid) were eluted with salt. The carbohydrate composition of each fraction was determined by using high pH anion-exchange chromatography. The sugar composition of the fractions was consistent with the presence of O-linked saccharides. No mannose was detected, suggesting that N-linked structures were absent. Calculations based on the relative amounts of GalNAc-ol showed that the neutral and sialylated species were most abundant (49% and 40%, respectively), and a significant fraction of the saccharides (11%) was sulfated.

**NMR Spectroscopy of MG2-T90 Oligosaccharides.** The reported proton NMR spectra of a large number of O-linked glycans compose a database of the chemical shifts of protons in the oligosaccharides. These chemical shifts are very sensitive to the presence of the immediate saccharide neighbors but are usually much less sensitive to more distant residues. Therefore, they are indicative of structural motifs rather than the complete oligosaccharide structure. We used both 1-D and 2-D (DQF-COSY) proton NMR spectroscopy to obtain information about the structural motifs in the unfractionated mixture of MG2-T90 O-linked oligosaccharides. The 1-D NMR spectra provided the highest sensitivity, but in some areas crowding precluded positive identification of important signals. DQF-COSY, which is less sensitive, resolved these signals; groups of cross-peaks with a characteristic fine structure permitted identification of the same type of structural reporter group within multiple environments.

1-D NMR spectroscopy of MG2-T90 oligosaccharides at 25 and 52 °C (Figure 2A) showed two prominent terminal structures. NeuAc linked  $\alpha 2 \rightarrow 3$  to Gal was revealed by peaks from  $H_{3eq}$  and  $H_{3ax}$  at 2.76 and 1.80 ppm, respectively, and a peak from  $CH_3-NAC$  at 2.032. Typical cross-peaks in the 2-D DQF-COSY spectrum involving  $H_{3eq}$  and  $H_{3ax}$  confirmed this assignment and demonstrated that NeuAc H4 resonated at 3.68 ppm (Figure 2B; Table 1). Fuc linked  $\alpha 1 \rightarrow 3$  to GlcNAc, another prominent terminal saccharide, was revealed in the 1-D spectra by a typical doublet from  $CH_3$  at 1.18 ppm, a peak from H1 at 5.11 ppm, and a characteristically downfield shifted peak from H5 at around 4.80 ppm (Figure 2A). The latter peak was obscured by HDO at 25 °C but was seen at 52 °C. The Fuc H5 and  $CH_3$  were also demonstrated by a very strong cross-peak in the DQF-COSY spectrum (Figure 2C; Table 1). The DQF-COSY spectrum also showed cross-peaks from Gal and GlcNAc that were characteristic for NeuAc $\alpha 2 \rightarrow 3$ Gal $\beta$ -, Gal $\beta 1 \rightarrow 4$ [Fuc $\alpha 1 \rightarrow 3$ ]GlcNAc- (Le<sup>x</sup>), and NeuAc $\alpha 2 \rightarrow 3$ Gal $\beta 1 \rightarrow 4$ [Fuc $\alpha 1 \rightarrow 3$ ]GlcNAc- (sLe<sup>x</sup>) determinants, as well as unsubstituted Gal $\beta 1 \rightarrow 4$ GlcNAc and Gal $\beta 1 \rightarrow 3$ GalNAc-ol (Figure 2D, Table 1). The absence of signals between 5.00 and 5.08 ppm, characteristic of Fuc H1 of Le<sup>a</sup>-containing structures, rules out the presence of this determinant (Gal $\beta 1 \rightarrow 3$ [Fuc $\alpha 1 \rightarrow 4$ ]GlcNAc). These and all of the following interpretations are in agreement with the published NMR spectra for the proposed structures (40, 41).

With regard to the core structures, peaks from GalNAc-ol were most informative. In the 1-D spectrum, a strong, well-isolated signal from H2 of GalNAc-ol was found at 4.39 ppm (Figure 2A; Table 1). This was a characteristic of both

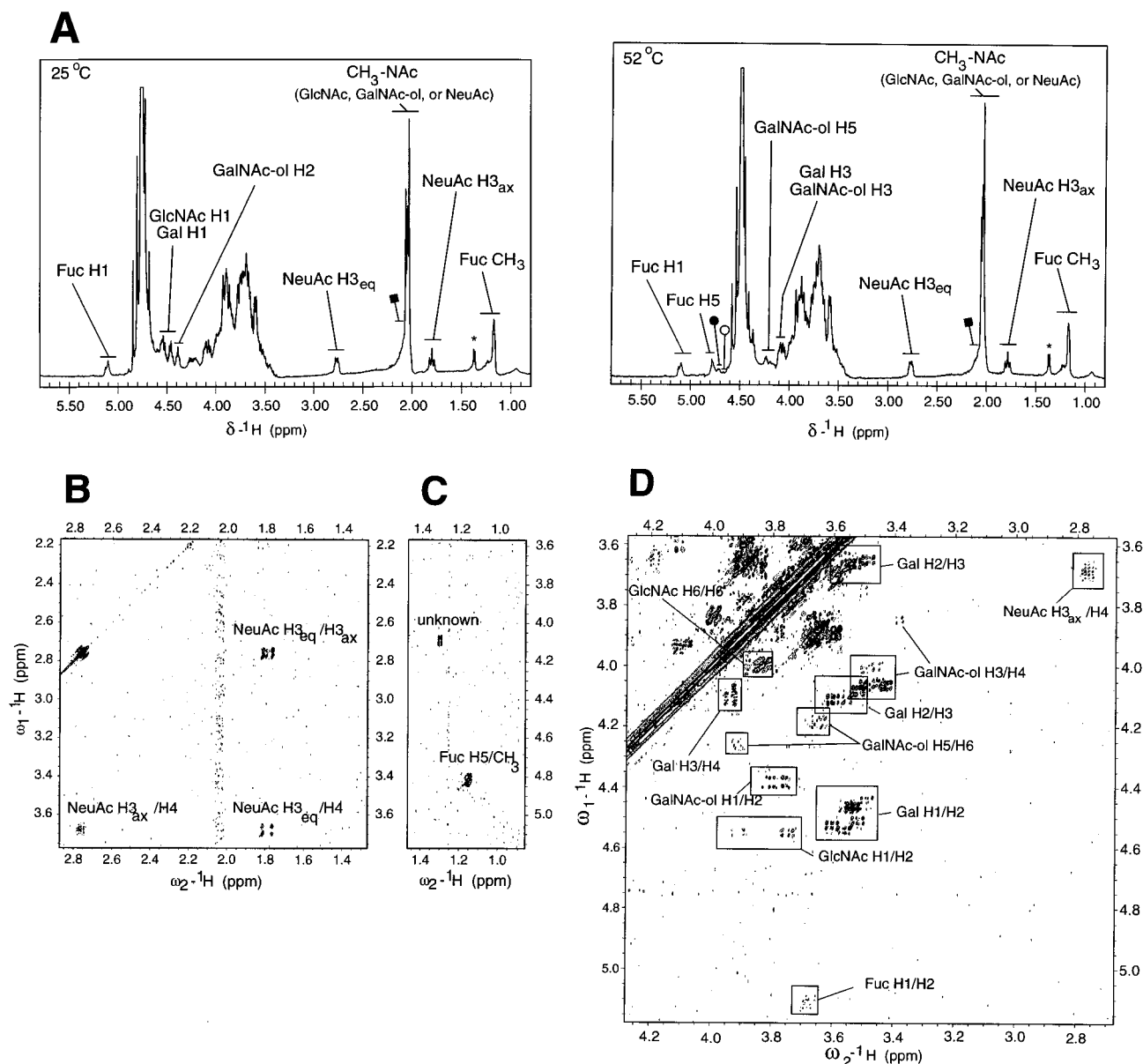


FIGURE 2: Structural reporter group regions of the 1-D and 2-D (DQF-COSY) NMR spectra of the total mixture of MG2-T90 oligosaccharides. O-Linked oligosaccharides were released from MG2-T90 by reductive  $\beta$ -elimination in 0.05 M NaOH/1 M NaBH<sub>4</sub>, desalted on Dowex 50WX8, and transferred to D<sub>2</sub>O (see Experimental Procedures). Panel A: 1-D spectra recorded at 25 (top) and 52 °C (bottom). The assignments of the major resolved signals are indicated. The open circle, filled circle, and filled square indicate signals discussed in the text. Panels B–D: 2-D DQF-COSY spectra of the same oligosaccharide sample recorded at 25 °C; three regions of the spectrum are shown. The assignments of cross-peaks are indicated (see also detailed assignments in Table 1). The peak labeled with an asterisk in panel A and the signal labeled as unknown in panel C are probably non-carbohydrate contaminants. Abbreviations: Fuc, fucose; Gal, galactose; GlcNAc, *N*-acetylglucosamine; GalNAc-ol, *N*-acetylgalactosaminitol; NeuAc, *N*-acetylneuraminic acid.

core 1 (Gal $\beta$ 1 $\rightarrow$ 3GalNAc-ol) and core 2 (Gal $\beta$ 1 $\rightarrow$ 3[GlcNAc $\beta$ 1 $\rightarrow$ 6]GalNAc-ol) containing structures. Other peaks from GalNAc-ol were better resolved in the DQF-COSY (Figure 2D; Table 1). Cross-peaks between H5 and H6 of GalNAc-ol confirmed the presence of core 1- and core 2-based structures, as did cross-peaks from H3 and H4 of GalNAc-ol, particularly easy to identify by their typical fine structure and high intensity. Multiple H3/H4 cross-peaks were found within the area typical of core 2 (shown as a range of chemical shift in Table 1), but these were slightly shifted depending on their outer structures. A similar peak at 3.85/3.39 ppm may be from H3/H4 of unsubstituted GalNAc-ol.

Because core 3- and core 4-based oligosaccharides are common motifs found in MG1 (48), we examined the NMR spectra of MG2-T90 oligosaccharides for evidence of these structures. For example, we were interested in diagnostic peaks in the 1-D spectrum (Figure 2A), such as H1 and CH<sub>3</sub>-NAc of the GlcNAc $\beta$ 1 $\rightarrow$ 3, in these cores that were not obscured by signals from the main structures. These peaks occur in combinations of  $\sim$ 4.65/2.07 and  $\sim$ 4.60/2.08 ppm, depending on the nature of additional substituents. The spectrum taken at 52 °C indicated that the first combination was a very minor component; in the 4.65 ppm region only a very small signal at 4.67 ppm was seen (Figure 2A, open circle). The latter combination was also a very minor

Table 1: Assignments of Signals (ppm) in <sup>1</sup>H NMR Analysis of the Glycitol Mixture Released from MG2<sup>a</sup>

GalNAc-ol	GalNAc-ol (A) R <sub>1</sub> -Galβ1-3GalNAc-ol (B) R <sub>1</sub> -Galβ1-3[4-R <sub>2</sub> -3-R <sub>3</sub> -GlcNAcβ1-6]GalNAc-ol (C)		
	A	B	C
H1		3.82	3.82
H1'		3.77	3.76
H2		4.39	4.39
H3	3.85	4.07	4.060–4.070
H4	3.39	3.50	3.420–3.510
H5		4.19	4.27
H6		3.66	3.92
NAc	2.06	2.044–2.050	2.063–2.068

Gal	Galβ1-3GalNAc-ol, Galβ1-4GlcNAc (A) Galβ1-4[Fucα1-3]GlcNAc (B) NeuAcα2-3Galβ1-3GalNAc-ol (C) NeuAcα2-3Galβ1-4GlcNAc (D) NeuAcα2-3Galβ1-4[Fucα1-3]GlcNAc (E)				
	A	B	C	D	E
H1	4.46	4.44	4.53	4.54	4.52
H2	3.54	3.50	3.60	3.57	3.52
H3	3.67	3.65	4.11	4.11	4.08
H4			3.95	3.93	3.93

GlcNAcβ1-6	4-R <sub>2</sub> -GlcNAcβ1-6GalNAc-ol (A) 4-R <sub>2</sub> -[Fucα1-3]GlcNAcβ1-6GalNAc-ol (B)	
	A	B
H1	4.55	4.55
H2	3.75	3.92
H6		~4.00
H6'		~3.83
NAc	2.060–2.067	2.053–2.056

R <sub>1</sub> -Galβ1-4[Fucα1-3]GlcNAc		NeuAcα2-3Gal	
Fuc		NeuAc	
H1	5.11	H3 <sub>ax</sub>	1.80
H2	3.68	H3 <sub>eq</sub>	2.76
H5	4.81	H4	3.68
CH <sub>3</sub>	1.18	NAc	2.03

<sup>a</sup> The reporter group from each type of saccharide residue (bold) is presented in a separate subtable with different columns for different structural contexts (A, B, C, etc.). R<sub>1</sub> is H or NeuAcα, R<sub>2</sub> is Galβ or NeuAcα2-3Galβ, and R<sub>3</sub> is H or Fucα. The chemical shift values (except for NAc) were determined from the cross-peaks identified by DQF-COSY at 25 °C (Figure 2, panels B–D). Each value given represents a range of about ±0.01 ppm because most cross-peaks derive from more than one compound and, hence, are slightly broadened due to this heterogeneity.

component, revealed by a downfield shoulder on the main CH<sub>3</sub>–NAc signal (Figure 2A, filled square). If larger amounts were present, a CH<sub>3</sub>–NAc signal, in addition to the farthest downfield signal from the main structure at 2.065 ppm, would be readily visible. Such a signal was missing in all the MG2-T90 spectra. Finally, cross-peaks in the 2-D spectra resembling those from H3/H4 of GalNAc-ol at ~4.00/3.50 ppm, typical of core 3 and core 4 structures, were barely detectable (Figure 2D). Thus, core 3- and 4-based structures are only minor components.

Taken together, the NMR data indicated that the following three motifs were prominent in the MG2-T90 oligosaccharide mixture: core 1 with NeuAc linked α2→3 to Gal (sialyl-T antigen); core 2 with Galβ1→4[Fucα1→3]GlcNAc (Le<sup>x</sup>), and core 2 with NeuAcα2→3Galβ1→4[Fucα1→3]GlcNAc (sLe<sup>x</sup>). Core 2 structures without either NeuAc or Fuc or both were also prominent.

**Mass Spectrometry of MG2-T90 Oligosaccharides.** First, we analyzed the permethylated neutral and *N,N*-dimethylsialic acid-containing saccharides by using GC–EIMS. The mobility and mass spectra of most of the components detected revealed structures consistent with those obtained from the NMR data. Panels A and B of Figure 3 show the total ion chromatograms of the permethylated neutral (N) and sialylated (S) species, respectively. Compound N1.1 was GalNAc-ol; N2.1, N3.1, N4.2, N5.2, N6.1, N6.2, N7.1, N7.2, S3.1, and S4.2 were saccharides with core 1-based structures; and N3.2, N4.1, N5.1, S4.1, S5.1, S5.2, S6.1, S6.2, S6.3, and S7.1 were saccharides with core 2-based structures.

The EI mass spectrum of the major saccharide that carried a sLe<sup>x</sup> determinant (Figure 3B, peak S6.2) is shown in Figure 3C. The figure also shows a diagram of this hexasaccharide (*M* = 1509) and formation of the fragment ions we detected. The cleavages we observed were consistent with the fragmentation patterns of permethylated O-linked oligosaccharides we published previously (49). Dimethyl amides, formed from the carboxyl groups of sialic acid residues (32), are characterized by intense fragment ions due to loss of the amide side groups (*m/z* 72, 1013–72). Other features in the mass spectrum included oxonium fragment ions and fragment ions from cleavages within the permethylated *N*-acetylgalactosaminitol residues. Charge retention on reducing (*m/z* 899, 1304) and nonreducing (*m/z* 189, 389, 1013) termini gave unequivocal evidence for a sequence as in the NeuAcα2→3Galβ1→4[Fucα1→3]GlcNAc (sLe<sup>x</sup>) determinant.

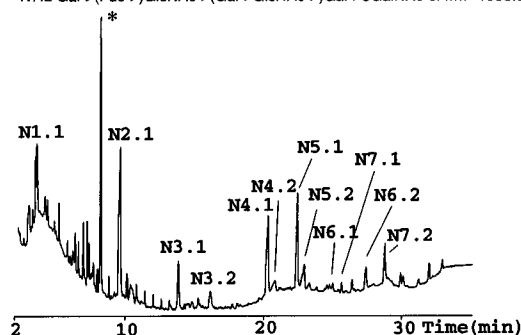
Due to its inherently greater sensitivity, GC–MS analysis also identified compounds that were not clearly revealed by NMR spectroscopy. For example, the mobility, mass, and fragment ions of N3.1, N6.1, and N7.1 indicated that they contained Fucα1→2Gal. In NMR spectra, this motif typically gives signals above 5.20 ppm for Fuc H1 and above 1.20 ppm for Fuc CH<sub>3</sub>. In 1-D NMR spectra of MG2-T90 oligosaccharides, the former signal was not detected. One or more minor peaks above 1.2 ppm may be due to the latter signal (Figure 2A). In 2-D NMR spectra the cross-peak for H5 and CH<sub>3</sub> of the Fucα1→2Gal motif was not detected. Therefore, saccharides containing this residue are probably minor components. Other oligosaccharides detected by GC–MS, but not by NMR, included N4.2, N5.2, N6.1, N7.1, N7.2, and S4.2 (see Figure 3A,B).

Second, we perdeuteracetylated the fraction of MG2-T90 oligosaccharides that contained sulfate (11%) and analyzed the products by FABMS. The mass of these compounds [*M* – H]<sup>–</sup> permitted calculation of their saccharide composition but not their sequence (Figure 3D). The data were consistent with the presence of the same major core structures as in the neutral and sialylated fractions. Hence, the peak at *m/z* 779 probably arose from a core 1 disaccharide with one sulfate group, the peak at *m/z* 1370 from a core 2 tetrasaccharide with one sulfate group, and the peak at *m/z* 1606 from a fucosylated core 2 saccharide with a Le<sup>x</sup> determinant and one sulfate group. Peaks corresponding to sulfated oligosaccharides with sialic acid were not detected.

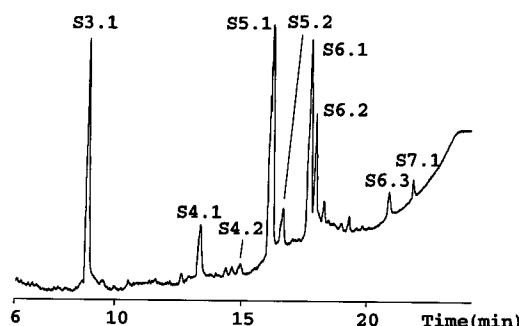
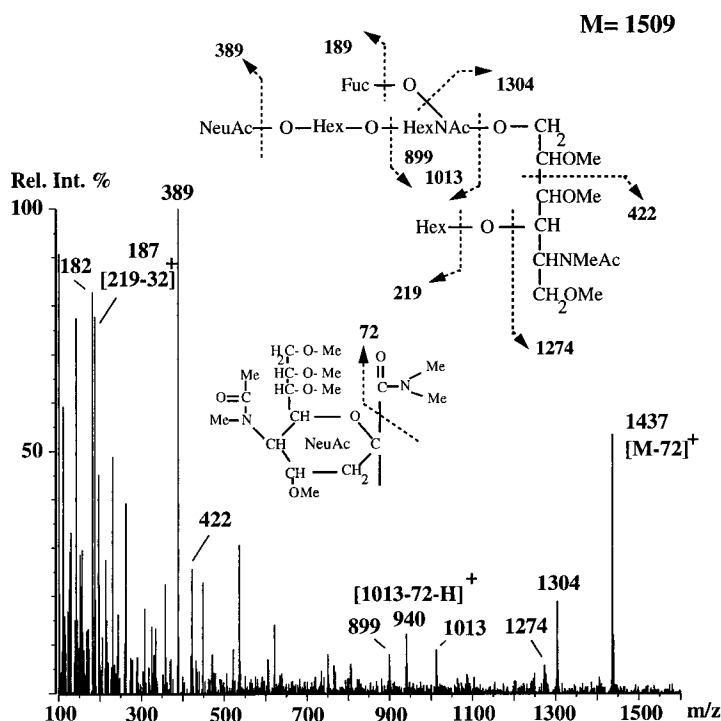
Finally, we used MALDI-TOFMS to determine the composition of the underivatized and the permethylated neutral and sialylated oligosaccharide fractions. In addition to the saccharides that were detected by GC–MS, this technique also detected lower-abundance or higher-molecular-weight saccharides, or both (Table 2). The results were

**A. (neutral)**

N1.1 GalNAc-ol Mw=307.2  
 N2.1 Gal→3GalNAc-ol Mw=511.3  
 N3.1 Fuc→Gal→3GalNAc-ol Mw=685.4  
 N3.2 Gal→3(GlcNAc→6)GalNAc-ol Mw=756.4  
 N4.1 Gal→3(Gal→4GlcNAc→6)GalNAc-ol Mw=960.5  
 N4.2 Gal→4GlcNAc→Gal→3GalNAc-ol Mw=960.5  
 N5.1 Gal→3(Gal→4(Fuc→)GlcNAc→6)GalNAc-ol Mw=1134.6  
 N5.2 Gal→4(Fuc→)GlcNAc→Gal→3GalNAc-ol Mw=1134.6  
 N6.1 Fuc→Gal→4(Fuc→)GlcNAc→Gal→3GalNAc-ol Mw=1308.7  
 N6.2 Gal→GlcNAc→(Gal→GlcNAc→(Fuc→)Gal→3GalNAc-ol Mw=1409.7  
 N7.1 Fuc→Gal→(Fuc→)GlcNAc→(Fuc→)Gal→3GalNAc-ol Mw=1482.8  
 N7.2 Gal→(Fuc→)GlcNAc→(Gal→GlcNAc→)Gal→3GalNAc-ol Mw=1583.8

**B. (sialylated)**

S3.1 NeuAc→Gal→3GalNAc-ol Mw=885.5  
 S4.1 NeuAc→Gal→3(GlcNAc→6)GalNAc-ol Mw=1130.6  
 S4.2 NeuAc→Gal→3(NeuAc→6)GalNAc-ol Mw=1259.7  
 S5.1 NeuAc→Gal→3(Gal→GlcNAc→6)GalNAc-ol Mw=1334.7  
 S5.2 Gal→3(NeuAc→Gal→GlcNAc→6)GalNAc-ol Mw=1334.7  
 S6.1 NeuAc→Gal→3(Gal→4(Fuc→)GlcNAc→6)GalNAc-ol Mw=1508.8  
 S6.2 Gal→3(NeuAc→Gal→(Fuc→)GlcNAc→6)GalNAc-ol Mw=1508.8  
 S6.3 NeuAc→Gal→3(NeuAc→Gal→GlcNAc→6)GalNAc-ol Mw=1708.9  
 S7.1 NeuAc→Gal→3(NeuAc→Gal→(Fuc→)GlcNAc→6)GalNAc-ol Mw=1883.0

**C. EI mass spectrum of peak S6.2****D. (sulfated)**

	[M-H] <sup>-</sup>
SF1 SO <sub>3</sub> <sup>-</sup> , Hex, HexNAc-ol	779
SF2 SO <sub>3</sub> <sup>-</sup> , Hex <sub>2</sub> , HexNAc, HexNAc-ol	1370
SF3 SO <sub>3</sub> <sup>-</sup> , Fuc, Hex <sub>2</sub> , HexNAc, HexNAc-ol	1606

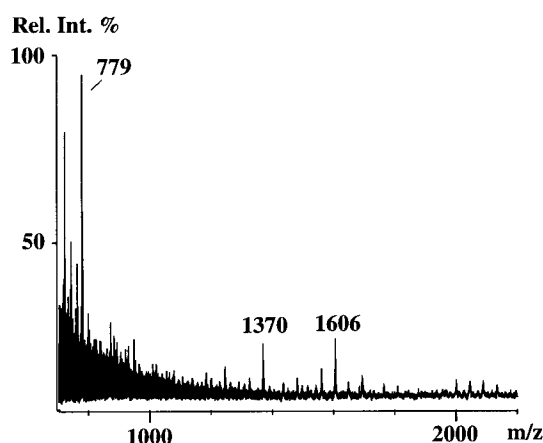


FIGURE 3: Mass spectra of MG2-T90 oligosaccharides. The oligosaccharides were analyzed by GC-EIMS. Panels A and B show the total ion chromatograms of the permethylated neutral (N) and sialylated (S) species, respectively, as well as the proposed saccharide composition of the major peaks. Only linkage positions that were clearly identified are indicated (43). The peak labeled with an asterisk in panel A is phthalate, a contaminant from plasticware. Panel C is an EI mass spectrum of the major saccharide that carried a sLe<sup>x</sup> determinant (peak S6.2, panel B). A diagram depicting formation of the major fragment ions is included. Panel D shows a mass spectrum, obtained by fast atom bombardment, of the perdeuterated sulfated oligosaccharide fraction and the proposed composition of the major species.

consistent with extended core 1- and core 2-based structures carrying one or more Fuc or NeuAc residues, or both. The NMR spectra did not identify these compounds specifically, but they did give some useful constraints. Compounds containing the GlcNAcβ1→3Gal motif were relatively minor, as indicated by the small size of the peak at about 4.70 ppm from GlcNAc H1 (Figure 2A, filled circle). Most of the Fuc and NeuAc in these compounds was linked to the 3-position of GlcNAc and Gal, respectively.

**Proposed Structures of the Major MG2-T90 Oligosaccharides.** Taken together, the NMR spectroscopy and mass spectrometry data revealed the major MG2 O-linked oligosaccharides to be the sialylated structures shown in Table 3 and their neutral, nonsialylated counterparts. These included the sialyl-T antigen (NeuAcα2→3Galβ1→3GalNAc-ol; S3.1), a core 2 pentasaccharide that also carried this motif (S5.1), a core 2 hexasaccharide with a Le<sup>x</sup> determinant [Galβ1→4(Fucα1→3)GlcNAc; S6.1], and a core 2 hexa-

Table 2: Summary of MG2 O-Linked Saccharide Molecular Ions

compd	composition <sup>a</sup>	molecular ions detected ( <i>m/z</i> )		
		underivatized <sup>b</sup> (MNa <sup>+</sup> )	permethylated <sup>b</sup> (MH <sup>+</sup> )	perdeuteracetlylated <sup>c</sup> (M - H) <sup>-</sup>
N1.1	GalNAc-ol		307.2	
N2.1	Gal, GalNAc-ol		511.3	
N3.1	Fuc, Gal, GalNAc-ol		685.4	
N3.2	Gal, GlcNAc, GalNAc-ol		756.4	
S3.1	NeuAc, Gal, GalNAc-ol		885.5	
N4.1, N4.2	Gal <sub>2</sub> , GlcNAc, GalNAc-ol	774.0	960.5	
S4.1	NeuAc, Gal, GlcNAc, GalNAc-ol		1130.6	
N5.1, N5.2	Fuc, Gal <sub>2</sub> , GlcNAc, GalNAc-ol	919.9	1134.6	
N5.3	Gal <sub>3</sub> , GlcNAc, GalNAc-ol		1164.6	
S4.2	NeuAc <sub>2</sub> , Gal, GalNAc-ol		1259.7	
N6.1	Fuc <sub>2</sub> , Gal <sub>2</sub> , GlcNAc, GalNAc-ol		1308.7	
S5.1, S5.2	NeuAc, Gal <sub>2</sub> , GlcNAc, GalNAc-ol	1064.9	1334.7	
N6.3	Fuc, Gal <sub>3</sub> , GlcNAc, GalNAc-ol		1338.7	
N6.2	Gal <sub>3</sub> , GlcNAc <sub>2</sub> , GalNAc-ol	1139.2	1409.7	
N7.1	Fuc <sub>3</sub> , Gal <sub>2</sub> , GlcNAc, GalNAc-ol		1482.8	
S6.1, S6.2	NeuAc, Fuc, Gal <sub>2</sub> , GlcNAc, GalNAc-ol	1210.9	1508.8	
N7.3	Fuc <sub>2</sub> , Gal <sub>3</sub> , GlcNAc, GalNAc-ol		1512.8	
N7.2	Fuc, Gal <sub>3</sub> , GlcNAc <sub>2</sub> , GalNAc-ol	1285.3	1583.8	
N7.4	Gal <sub>4</sub> , GlcNAc <sub>2</sub> , GalNAc-ol		1613.8	
S7.2	NeuAc, Fuc <sub>2</sub> , Gal <sub>2</sub> , GlcNAc, GalNAc-ol	1356.9	1682.9	
S6.3	NeuAc <sub>2</sub> , Gal <sub>2</sub> , GlcNAc, GalNAc-ol		1708.9	
N8.1	Fuc <sub>2</sub> , Gal <sub>3</sub> , GlcNAc <sub>2</sub> , GalNAc-ol		1757.9	
N8.2	Fuc, Gal <sub>3</sub> , GlcNAc <sub>3</sub> , GalNAc-ol		1828.9	
S7.1	NeuAc <sub>2</sub> , Fuc, Gal <sub>2</sub> , GlcNAc, GalNAc-ol	1501.9	1883.0	
S8.1	NeuAc, Fuc, Gal <sub>3</sub> , GlcNAc <sub>2</sub> , GalNAc-ol	1576.8	1958.0	
N9.2	Gal <sub>5</sub> , GlcNAc <sub>3</sub> , GalNAc-ol		2063.0	
N10.1	Fuc <sub>2</sub> , Gal <sub>4</sub> , GlcNAc <sub>3</sub> , GalNAc-ol	1795.5	2207.1	
N10.2	Fuc, Gal <sub>5</sub> , GlcNAc <sub>3</sub> , GalNAc-ol		2237.1	
N9.1	Fuc, Gal <sub>4</sub> , GlcNAc <sub>4</sub> , GalNAc-ol		2278.2	
N11.1	Fuc <sub>3</sub> , Gal <sub>4</sub> , GlcNAc <sub>3</sub> , GalNAc-ol		2381.2	
S10.1	NeuAc, Fuc, Gal <sub>4</sub> , GlcNAc <sub>3</sub> , GalNAc-ol	1940.6	2407.2	
S11.1	NeuAc, Fuc <sub>2</sub> , Gal <sub>4</sub> , GlcNAc <sub>3</sub> , GalNAc-ol	2087.1	2581.3	
S11.2	NeuAc <sub>2</sub> , Fuc, Gal <sub>4</sub> , GlcNAc <sub>3</sub> , GalNAc-ol		2781.4	
S12.1	NeuAc <sub>2</sub> , Fuc <sub>2</sub> , Gal <sub>4</sub> , GlcNAc <sub>3</sub> , GalNAc-ol		2955.5	
SF1	SO <sub>3</sub> , Gal, GalNAc-ol			779
SF2	SO <sub>3</sub> , Gal <sub>2</sub> , GlcNAc, GalNAc-ol			1370
SF3	SO <sub>3</sub> , Fuc, Gal <sub>2</sub> , GlcNAc, GalNAc-ol			1606

<sup>a</sup> The following assumptions have been made: hexose residues are galactose, *N*-acetylhexosamine residues are *N*-acetylglucosamine, deoxyhexose residues are fucose, and *N*-acetylhexosaminitol residues are *N*-acetylgalactosaminitol. <sup>b</sup> Analyzed by MALDI-TOFMS. <sup>c</sup> Analyzed by FABMS.

saccharide with a sLe<sup>x</sup> determinant (NeuAcα2→3Galβ1→4[Fucα1→3]GlcNAc; S6.2). Interestingly, saccharides that contained the B determinant were not detected, although the donor was a secretor with blood type B. This finding is in agreement with our previous study which showed that the A, B, H, Le<sup>a</sup>, and Le<sup>b</sup> blood group determinants are carried primarily by MG1 (50).

*sLe<sup>x</sup> Is Expressed by MG2 of Most, but Not All, Individuals.* Since the foregoing structural analyses were performed on MG2-T90 isolated from a single donor, we were interested in knowing whether the prominent oligosaccharide motifs we identified are a special feature of MG2 in this particular sample or are commonly expressed. To answer this question, nitrocellulose replicas of electrophoretically separated SMSL or whole saliva samples were stained with anti-sLe<sup>x</sup> [CSLEX-1 (51)]. Results typical of those we obtained are shown in Figure 4A. In 31 of 32 samples analyzed, a band with the same relative electrophoretic mobility as MG2 was the major antibody-reactive species. However, we observed variations in band width and staining intensity, as well as in the electrophoretic mobility, of the MG2 in these samples. Antibody binding to higher-molecular-weight components (*M<sub>r</sub>* > 120 000), which likely included MG1, was also detected. Bands with *M<sub>r</sub>* < 120 000 (lanes 1, 3, and 9) were due to nonspecific reactivity with the secondary antibody

alone. Interestingly, we failed to detect antibody binding to any salivary components of one of the 32 individuals (Figure 4A, lane 7). We obtained essentially the same results when we probed replicas of the same samples with a different antibody that also specifically recognizes the sLe<sup>x</sup> epitope [2H-5 (52), data not shown].

To determine whether similar amounts of MG2 were present in the saliva samples, we stained identical nitrocellulose replicas with jacalin, a lectin that binds mono- or disialylated structures carrying Galβ1→3GalNAc (53), a motif found in the major MG2-T90 saccharides (Table 3). A band with the same relative electrophoretic mobility as MG2 reacted with this lectin in all the salivas tested, including the sLe<sup>x</sup>-negative sample (Figure 4B, lane 7). This suggested that at least some of the individual differences in the MG2 staining pattern were due to variations in the number of sLe<sup>x</sup> epitopes the molecules carried. Staining replicas of the same samples with wheat germ agglutinin, a lectin that reacts with glycoproteins containing *N*-acetylglucosamine and sialic acid (54, 55), gave essentially the same results (data not shown).

*MG2 Is a Selectin Ligand.* L-, P-, and E-selectins belong to a group of cell adhesion molecules that are found on leukocytes or endothelial cells (56–60). The selectins have C-type lectin domains that mediate Ca<sup>2+</sup>-dependent adhesion



Table 3: Prominent MG2-T90 Saccharide Structures

compd	molecular mass	structure
S3.1	885.5	<div>GalNAc-ol /  Galβ1-3 /  NeuAcα2-3</div>
S5.1	1334.7	<div>Galβ1-4GlcNAcβ1-6 /  GalNAc-ol /  Galβ1-3 /  NeuAcα2-3</div>
S6.1	1508.8	<div>Galβ1-4GlcNAcβ1-6 /  Fucα1-3 /  Galβ1-3 /  NeuAcα2-3 /  GalNAc-ol</div>
S6.2	1508.8	<div>Galβ1-4GlcNAcβ1-6 /  NeuAcα2-3 /  Fucα1-3 /  Galβ1-3 /  GalNAc-ol</div>

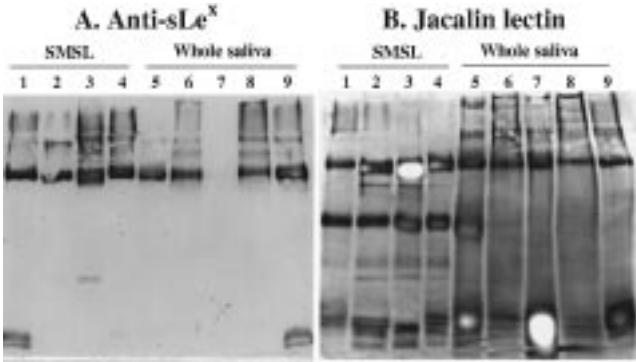


FIGURE 4: Sialyl Le<sup>x</sup> determinant expressed by MG2 of most, but not all, individuals. Panel A, a nitrocellulose replica of electrophoretically separated SMSL (lanes 1–4) and whole saliva (lanes 5–9) samples from different donors stained with a monoclonal antibody that specifically recognizes the sLe<sup>x</sup> epitope. All but one sample (lane 7) reacted with the antibody. Panel B, a nitrocellulose replica of the same samples stained with jacalin, a lectin that binds mono- or disialylated structures carrying Galβ1–3GalNAc. A band of the same *M<sub>r</sub>* as MG2 reacted with this lectin in all the lanes.

by recognizing specific carbohydrate sequences, including sLe<sup>x</sup> tetrasaccharides and related structures (56, 57, 59–61). This class of adhesive interactions plays a particularly important role in immune functions. For example, L-selectin on leukocytes binds to glycoprotein receptors that carry sLe<sup>x</sup> motifs present on high endothelial venules (GlyCAM-1, CD34, and Sgp200), a critical early step in homing. Since sLe<sup>x</sup> was a prominent feature of MG2 saccharides, we asked whether MG2 exhibited selectin ligand activity. First, we assayed the ability of an L-selectin/Ig chimera to bind to purified MG2 coated onto wells of Immulon 2 plates.

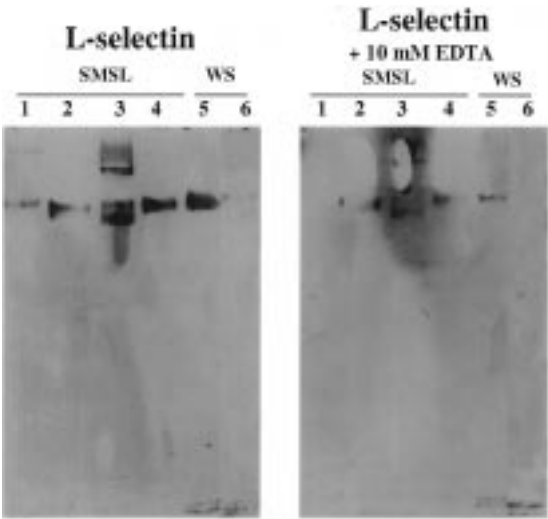


FIGURE 5: Nitrocellulose replicas of electrophoretically separated SMSL (lanes 1–4) and whole saliva (WS, lanes 5 and 6) samples overlaid with a preformed complex of L-selectin/human IgG chimera, biotinylated goat anti-human IgG, and streptavidin–alkaline phosphatase, in the absence (left) and the presence (right) of EDTA. The selectin-reactive bands were visualized by staining the replicas with alkaline phosphatase substrate. All the samples that reacted with anti-sLe<sup>x</sup> (see Figure 4) bound the L-selectin chimera (lanes 1–5); the sample that failed to interact with the antibody (see Figure 4, panel B, lane 7) interacted weakly with the chimera (lane 6).

Significant binding was detected, reaching an OD of ~1 after 30 min. Addition of 10 mM EDTA reduced binding by ~85%. Second, we assayed binding of the L-selectin/Ig chimeras to nitrocellulose replicas of electrophoretically separated SMSL (Figure 5, lanes 1–4) or whole saliva (Figure 5, lanes 5 and 6) samples. MG2 in most samples interacted with L-selectin (lanes 1–5). Significantly less binding was observed in the presence of 10 mM EDTA. A high-molecular-weight band in some saliva samples, probably MG1, also supported L-selectin binding (Figure 5, lane 3). In comparison, the saliva sample that did not stain with anti-sLe<sup>x</sup> (Figure 4, lane 7) supported a very low level of L-selectin binding that is barely detectable in the photograph (Figure 5, lane 6).

DISCUSSION

The structural data presented here show that Le<sup>x</sup> and sLe<sup>x</sup> determinants are prominent motifs carried by human MG2 O-linked oligosaccharides from a single individual. These results led us to predict a novel function for this molecule, namely, that MG-2, like other mucin-type glycoproteins that carry these carbohydrate structures, is a selectin ligand (56, 59, 60, 62). To begin to test this hypothesis, we assayed the ability of MG2 in saliva samples from 32 individuals to interact with anti-sLe<sup>x</sup>. In 31 of the 32 samples analyzed, the low-molecular-weight mucin bound the antibody, as did higher-molecular-weight components (>*M<sub>r</sub>* 120 000) which likely included MG1; one sample contained MG2, but had no antibody-reactive bands. In the former samples, MG2 and occasionally MG1 reacted with the L-selectin chimeras; in the latter sample, little L-selectin binding was detected. Together, these data suggest that MG2 has selectin ligand activity but that its ability to bind selectin is lost in some individuals, probably due to changes in glycosylation.

There have been two previous studies of human salivary mucin carbohydrate structures. In the first, Reddy et al. (63) purified MG2 and then used a combination of gel filtration, paper chromatography, and high-voltage paper electrophoresis to characterize its oligosaccharides. Seven different structures were proposed, of which ~80% had type 1 cores and were either disaccharides or trisaccharides with terminal NeuAc or Fuc. The remaining structures had type 2 cores with 5–7 saccharides in toto, and the termini carried either Le<sup>x</sup> (Gal $\beta$ 1→4[Fuc $\alpha$ 1→3]GlcNAc) or Le<sup>y</sup> ([Fuc $\alpha$ 1→2]-Gal $\beta$ 1→4[Fuc $\alpha$ 1→3]GlcNAc) determinants. In contrast, the structural data presented here were acquired by using a combination of NMR and mass spectrometry techniques. Le<sup>x</sup> termini were among the major motifs detected, but saccharides carrying Fuc $\alpha$ 1→2Gal sequences were minor components. Differences in the analytical approaches used in the former and the present study are likely to account for discrepancies in the conclusions.

In the second study, Klein et al. (48) used whole saliva collected from 20 donors (blood type O) as the starting material. The samples were pooled and digested with Pronase. A high-molecular-weight fraction ( $M_r \geq 320\,000$ ), which had the chemical composition of mucin glycopeptides, was isolated by chromatography on a CL-2B column. The O-linked saccharides were released by alkaline borohydride treatment; a subfraction of the neutral and sialylated species was analyzed by using a combination of NMR and FAB/MS. Of the 37 structures identified, many were core 3- (GlcNAc $\beta$ 1→3GalNAc) and core 4-based (GlcNAc $\beta$ 1→3-[GlcNAc $\beta$ 1→6]GalNAc) structures, with 2–6 sugar residues and a wide variety of termini that included H, Le<sup>x</sup>, Le<sup>y</sup>, Le<sup>a</sup>, and Le<sup>b</sup> determinants. Most of the monosialylated species contained terminal NeuAc linked  $\alpha$ 2→6 to GalNAc-ol. Only a minor fraction of these oligosaccharides was among the MG2 structures reported here, and no sLe<sup>x</sup> termini were detected. These discrepancies probably reflect differences in the starting material used; the chemical composition of the glycopeptide fraction studied by Klein et al. (48) was similar to that of MG1 (24, 25), whereas the present study used purified MG2. Together, the results of both studies suggest that MG1 and MG2, whose core tandem repeats have distinct peptide sequences (19, 23), also carry very different carbohydrate structures. This finding is consistent with recently published information about the specificity of the transferases that initiate O-glycan acquisition (64–67), as well as with data that suggest that MG1 and MG2 are found in different subpopulations of SMSL-gland cells (68).

Our interest in MG2 structure arose from previous studies in which we investigated MG2 function. We and others have shown that this salivary mucin plays an important dual role in the oral cavity. As a pellicle component, MG2 coats enamel and cementum surfaces (27). MG2 is also a bacterial receptor. For example, we found that *Streptococcus sanguis* strains 72-40 and 10556 bind to intact MG2 immobilized on nitrocellulose membranes but not to desialylated MG2 or intact MG1 (13). This suggests that the streptococcal adhesins mediating this interaction recognize the NeuAc $\alpha$ 2→3 termini that are prominent among MG2 oligosaccharides, rather than the NeuAc $\alpha$ 2→6 epitope carried by MG1. In addition, we recently found that the same strains bind to MG2 regardless of whether the mucin carries sLe<sup>x</sup> (data not shown). This result, together with a previous study

showing that a trisaccharide, NeuAc $\alpha$ 2→3Gal $\beta$ 1→3GalNAc, significantly inhibits MG2–streptococcal interactions (69), suggests that the sialyl-T epitope may be the primary *S. sanguis* receptor. In contrast, we find that *Actinomyces naeslundii* bound desialylated but not intact MG2 (in preparation). This result is consistent with the work of Brennan et al. (70), who showed that *Actinomyces* strains bound glycosphingolipids carrying terminal Gal $\beta$ 1→3GalNAc sequences. *Actinomyces* strains and a number of other oral bacteria possess potent sialidase activity (71, 72), one possible explanation of how MG2 with terminal Gal $\beta$ 1→3GalNAc sequences might be generated. Together, the results of these studies suggest that many of the bacteria studied to date adhere to MG-2 via oligosaccharides other than Le<sup>x</sup> and sLe<sup>x</sup>.

We had expected that analyzing the structure of MG2 oligosaccharides would help us to better understand how these carbohydrate receptors interact with bacteria. Our first indication that MG2 might have another function came when we found that Le<sup>x</sup> and sLe<sup>x</sup> epitopes were prominent among MG2 structures. All members of the selectin family (E-, L-, and P-selectin) can recognize the sLe<sup>x</sup> tetrasaccharide and related structures carried on mucin-like proteins (56, 60, 62). However, these carbohydrate sequences are commonly found on glycoproteins, most of which are not physiological selectin ligands. Therefore, additional structural criteria must determine whether a molecule can perform this important function. Although the exact structures carried by the naturally occurring selectin ligands are still largely unknown, several features of their carbohydrate residues are thought to contribute to high-affinity interactions. One such feature is the fine structure of the individual carbohydrate determinants carried by the ligands, for example, the GlyCAM-1 capping groups, 6'-sulfo-sLe<sup>x</sup> and 6-sulfo-sLe<sup>x</sup> (59). Another important factor is proper spacing or combining of the saccharide chains (73). Our data indicated that Le<sup>x</sup> and sLe<sup>x</sup> were prominent structural features of the MG2 saccharides. In addition, analysis of the sulfated fraction, which comprised about 10% of the total saccharides, suggested that this subset carried core structures (core 1, core 2, and fucosylated core 2) similar to those of the neutral and the sialylated fractions. Thus, the data suggested the presence of the sulfated Le<sup>x</sup> determinant among the MG2 saccharides. But the position of the sulfate group (e.g., 3'-sulfo-, 6-sulfo- or 6'-sulfo-Le<sup>x</sup>) could not be deduced from the present data. With regard to biological activity, it is interesting to note that one recent study (74) indicated that L-selectin bound at a higher affinity to 3'-sulfo-Le<sup>x</sup> determinants than to 3'-sialyl Le<sup>x</sup> determinants. In conclusion, it is likely that both sLe<sup>x</sup> and sulfated Le<sup>x</sup> determinants on the MG2 molecule contribute to the L-selectin binding. However, proper spacing or clustering of the saccharides, probably in a unique fashion, on the MG2 molecule is also likely to be critical for the selectin ligand activity of the molecule.

Our findings have important implications for oral health. It now seems likely that MG2 in the saliva of many individuals coats oral surfaces, where it may serve as both a bacterial receptor and a selectin ligand. Oral diseases linked to immune dysfunction or alterations in the oral flora are widespread in the population (e.g., periodontitis). It is conceivable that MG2 in the saliva of some individuals may lack one of these functions. In fact, a sample we studied

contained MG2 that failed to express sLe<sup>x</sup> and to act as a selectin ligand. Thus, alterations in MG2 glycosylation could result in a molecule that forms a pellicle that promotes bacterial adhesion but not leukocyte binding. In this case, the affected individual may be more susceptible to oral diseases, a hypothesis that will be tested in clinical studies.

## ACKNOWLEDGMENT

We would like to thank Niclas Karlsson for his technical support.

## REFERENCES

- Hatton, M. N., Loomis, R. E., Levine, M. J., and Tabak, L. A. (1985) *Biochem. J.* 230, 817–820.
- Aguirre, A., Mendoza, B., Levine, M. J., Hatton, M. N., and Douglas, W. H. (1989) *Arch. Oral Biol.* 34, 675–677.
- Gans, R. F., Watson, G. E., and Tabak, L. A. (1990) *Arch. Oral Biol.* 35, 487–492.
- Mandel, I. D. (1987) *J. Dent. Res.* 66, 623–627.
- Bennick, A., Chau, G., Goodlin, R., Abrams, S., Tustian, D., and Madapallimattam, G. (1983) *Arch. Oral Biol.* 28, 19–27.
- Fisher, S. J., Prakobphol, A., Kajisa, L., and Murray, P. A. (1987) *Arch. Oral Biol.* 32, 509–517.
- Al-Hashimi, I., and Levine, M. J. (1989) *Arch. Oral Biol.* 34, 289–295.
- Moreno, E. C., Kresak, M., and Hay, D. I. (1982) *J. Biol. Chem.* 257, 2981–2989.
- Moreno, E. C., Kresak, M., and Hay, D. I. (1984) *Calcif. Tissue Int.* 36, 48–59.
- Mellersh, A., Clark, A., and Hafiz, S. (1979) *Br. J. Vener. Dis.* 55, 20–23.
- Obenauf, S. D., Cowman, R. A., and Fitzgerald, R. J. (1986) *Infect. Immun.* 51, 440–444.
- Gillece-Castro, B. L., Prakobphol, A., Burlingame, A. L., Leffler, H., and Fisher, S. J. (1991) *J. Biol. Chem.* 266, 17358–17368.
- Murray, P. A., Prakobphol, A., Lee, T., Hoover, C. I., and Fisher, S. J. (1992) *Infect. Immun.* 60, 31–38.
- Scannapieco, F. A., Torres, G. I., and Levine, M. J. (1995) *J. Dent. Res.* 74, 1360–1366.
- Groenink, J., Ligtenberg, A. J., Veerman, E. C., Bolscher, J. G., and Nieuw, A. A. (1996) *Antonie van Leeuwenhoek* 70, 79–87.
- van der Spek, J. C., Wyandt, H. E., Skare, J. C., Milunsky, A., Oppenheim, F. G., and Troxler, R. F. (1989) *Am. J. Hum. Genet.* 45, 381–387.
- Azen, E. A., and Maeda, N. (1988) *Adv. Hum. Genet.* 17, 141–199.
- Maeda, N., Kim, H. S., Azen, E. A., and Smithies, O. (1985) *J. Biol. Chem.* 260, 11123–11130.
- Bobek, L. A., Tsai, H., Biesbrock, A. R., and Levine, M. J. (1993) *J. Biol. Chem.* 268, 20563–20569.
- Levine, M. J. (1993) *Crit. Rev. Oral Biol. Med.* 4, 279–286.
- Lamkin, M. S., and Oppenheim, F. G. (1993) *Crit. Rev. Oral Biol. Med.* 4, 251–259.
- Tabak, L. A. (1995) *Annu. Rev. Physiol.* 57, 547–564.
- Nielsen, P. A., Bennett, E. P., Wardall, H. H., Terkildsen, M. H., Hanibal, J., and Clausen, H. (1997) *Glycobiology* 7, 413–419.
- Levine, M. J., Reddy, M. S., Tabak, L. A., Loomis, R. E., Bergey, E. J., Jones, P. C., Cohen, R. E., Stinson, M. W., and Al, H. I. (1987) *J. Dent. Res.* 66, 436–441.
- Loomis, R. E., Prakobphol, A., Levine, M. J., Reddy, M. S., and Jones, P. C. (1987) *Arch. Biochem. Biophys.* 258, 452–464.
- Prakobphol, A., Levine, M. J., Tabak, L. A., and Reddy, M. S. (1982) *Carbohydr. Res.* 108, 111–122.
- Kajisa, L., Prakobphol, A., Schiodt, M., and Fisher, S. J. (1990) *Scand. J. Dent. Res.* 98, 461–471.
- Troxler, R. F., Offner, G. D., Zhang, F., Iontcheva, I., and Oppenheim, F. G. (1995) *Biochem. Biophys. Res. Commun.* 217, 1112–1119.
- Morrissey, J. H. (1981) *Anal. Biochem.* 117, 307–310.
- Jay, G. D., Culp, D. J., and Jahnke, M. R. (1990) *Anal. Biochem.* 185, 324–330.
- Reddy, M. S., Bobek, L. A., Haraszthy, G. G., Biesbrock, A. R., and Levine, M. J. (1992) *Biochem. J.* 287, 639–643.
- Karlsson, N. G., Karlsson, H., and Hansson, G. C. (1995) *Glycoconjugate J.* 12, 69–76.
- Hardy, M. R., Townsend, R. R., and Lee, Y. C. (1988) *Anal. Biochem.* 170, 54–62.
- Karlsson, N. G., and Hansson, G. C. (1995) *Anal. Biochem.* 224, 538–541.
- Rance, M., Sorensen, O. W., Bodenhausen, G., Wagner, G., Ernst, R. R., and Wuthrich, K. (1983) *Biochem. Biophys. Res. Commun.* 117, 479–485.
- Marion, D., and Wuthrich, K. (1983) *Biochem. Biophys. Res. Commun.* 113, 967–974.
- Basus, V. J., Billeter, M., Love, R. A., Stroud, R. M., and Kuntz, I. D. (1988) *Biochemistry* 27, 2763–2771.
- Kneller, D., and Kuntz, I. D. (1993) *Striker*, University of California, San Francisco.
- Day, M., and Kuntz, I. D. (1993) *Sparky: NMR Display and Analysis Program*, University of California, San Francisco.
- Kamerling, J. H., and Vliegenthart, J. F. G. (1992) in *Biological Magnetic Resonance* (Berliner, L. J., and Reben, J., Eds.) Plenum Press, New York and London.
- SUGABASE. <http://www.boc.chem.ruu.nl/sugabase/sugabase.html> (accessed 1997). A web site compiling published NMR data for saccharides currently up to 1994.
- Mohr, M. D., Bornsen, K. O., and Widmer, H. M. (1995) *Rapid Commun. Mass Spectrom.* 9, 809–814.
- Karlsson, H., Carlstedt, I., and Hansson, G. C. (1989) *Anal. Biochem.* 182, 438–446.
- Karlsson, N. G., Karlsson, H., and Hansson, G. C. (1996) *J. Mass Spectrom.* 31, 560–572.
- Laemmli, U. (1970) *Nature* 227, 680–685.
- Towbin, H., Staehelin, T., and Gordon, J. (1979) *Proc. Natl. Acad. Sci. U.S.A.* 76, 4350–4354.
- Bertozzi, C. R., Singer, M. S., and Rosen, S. D. (1997) *J. Immunol. Methods* 203, 157–165.
- Klein, A., Carnoy, C., Wieruszkeski, J. M., Strecker, G., Strang, A. M., van Halbeck, H., Roussel, P., and Lamblin, G. (1992) *Biochemistry* 31, 6152–6165.
- Hansson, G. C., and Karlsson, H. (1993) *Methods Mol. Biol.* 14, 47–54.
- Prakobphol, A., Leffler, H., and Fisher, S. J. (1993) *Crit. Rev. Oral Biol. Med.* 4, 325–333.
- Hirota, M., Fukushima, K., Terasaki, P. I., Terashita, G. Y., Galton, J., and Kawahara, M. (1985) *Cancer Res.* 45, 6453–6456.
- Takada, A., Ohmori, K., Yoneda, T., Tsuyuoka, K., Hasegawa, A., Kiso, M., and Kannagi, R. (1993) *Cancer Res.* 53, 354–361.
- Ahmed, H., and Chatterjee, B. P. (1989) *J. Biol. Chem.* 264, 9365–9372.
- Hellstrom, U., Dillner, M. L., Hammarstrom, S., and Perlmann, P. (1976) *J. Exp. Med.* 144, 1381–1385.
- Peters, B. P., Ebisu, S., Goldstein, I. J., and Flashner, M. (1979) *Biochemistry* 18, 5505–5511.
- Rosen, S. D., and Bertozzi, C. R. (1994) *Curr. Opin. Cell Biol.* 6, 663–673.
- Varki, A. (1994) *Proc. Natl. Acad. Sci. U.S.A.* 91, 7390–7397.
- Hemmerich, S., Butcher, E. C., and Rosen, S. D. (1994) *J. Exp. Med.* 180, 2219–2226.
- Hemmerich, S., Leffler, H., and Rosen, S. D. (1995) *J. Biol. Chem.* 270, 12035–12047.
- Sanders, W. J., Katsumoto, T. R., Bertozzi, C. R., Rosen, S. D., and Kiessling, L. L. (1996) *Biochemistry* 35, 14862–14867.
- Hemmerich, S., Bertozzi, C. R., Leffler, H., and Rosen, S. D. (1994) *Biochemistry* 33, 4820–4829.

62. Rosen, S. D. (1993) *Semin. Immunol.* 5, 237–247.
63. Reddy, M. S., Levine, M. J., and Prakobphol, A. (1985) *J. Dent. Res.* 64, 33–36.
64. Sorensen, T., White, T., Wandall, H. H., Kristensen, A. K., Roepstorff, P., and Clausen, H. (1995) *J. Biol. Chem.* 270, 24166–24173.
65. Bennett, E. P., Hassan, H., and Clausen, H. (1996) *J. Biol. Chem.* 271, 17006–17012.
66. Clausen, H., and Bennett, E. P. (1996) *Glycobiology* 6, 635–646.
67. Nehrke, K., Hagen, F. K., and Tabak, L. A. (1996) *J. Biol. Chem.* 271, 7061–7065.
68. Nielsen, P. A., Mandel, U., Therkildsen, M. H., and Clausen, H. (1996) *J. Dent. Res.* 75, 1820–1826.
69. Murray, P. A., Levine, M. J., Tabak, L. A., and Reddy, M. S. (1982) *Biochem. Biophys. Res. Commun.* 106, 390–396.
70. Brennan, M. J., Joralmmon, R. A., Cisar, J. O., and Sandberg, A. L. (1987) *Infect. Immun.* 55, 487–489.
71. Beighton, D., and Whiley, R. A. (1990) *J. Clin. Microbiol.* 28, 1431–1433.
72. Yeung, M. K. (1993) *Infect. Immun.* 61, 109–116.
73. Maaheimo, H., Renkonen, R., Turunen, J. P., Penttilä, L., and Renkonen, O. (1995) *Eur. J. Biochem.* 234, 616–625.
74. Galustian, C., Childs, R. A., Yuen, C. T., Hasegawa, A., Kiso, M., Lubineau, A., Shaw G., and Feizi, T. (1997) *Biochemistry* 36, 5260–5266.

BI972612A